

You Only Explain Once

David A. Kelly, Hana Chockler, Nathan Blake, Aditi Ramaswamy,
Melane Navaratnarajah, Aaditya Shivakumar
Department of Informatics
King’s College London

david.a.kelly, hana.chockler, nathan.blake, aditi.ramaswamy,
melane.navarathnarajah, aaditya.shivakumar AT kcl.ac.uk

Daniel Kroening
AWS
drk@amazon.co.uk

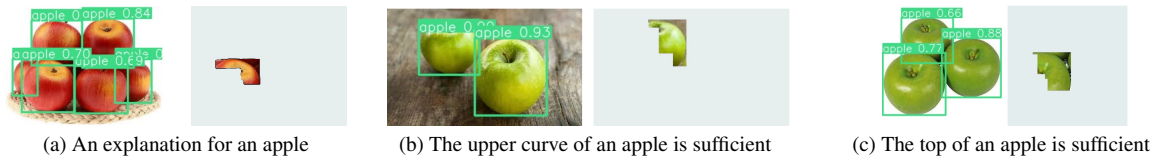


Figure 1. Three different explanations for an apple, provided by ANON-REX. While all explanations are strongly rectilinear, they reveal that only a section of an apple is sufficient for classification, regardless of color.

Abstract

In this paper, we propose a new black-box explainability algorithm and tool, ANON-REX, for efficient explanation of the outputs of object detectors. The new algorithm computes explanations for all objects detected in the image simultaneously. Hence, compared to the baseline, the new algorithm reduces the number of queries by a factor of $10\times$ for the case of ten detected objects. The speedup increases further with the number of objects. Our experimental results demonstrate that ANON-REX can explain the outputs of YOLO with a negligible overhead over the running time of YOLO. We also demonstrate similar results for explaining SSD and Faster R-CNN. The speedup is achieved by avoiding backtracking by combining aggressive pruning with a causal analysis.

1. Introduction

Neural networks are now a primary building block of most computer vision systems. The opacity of neural networks creates demand for explainability techniques, which attempt to provide insight into *why* a particular input yields a particular observed output. Beyond increasing a user’s confidence in the output, as well as their trust in the AI system, these insights help to uncover subtle recognition errors that are not detectable from the output alone [7].

Explainability is especially important for object detection. Object detectors are fast networks, localizing and identifying objects within a given image. Object detectors are crucial for self-driving vehicles and advanced driver-assistance systems, as well as many other applications, as they are fast enough to compute results in real time. The state of the art in the field is YOLO [21], an object detector that localizes and labels objects on an input image within one pass. Other notable object detectors include SSD [16], which is also a one-pass object detector, and a number of two-passes object detectors, most popular of which are the variants of R-CNN [12]. These are slower in general, but recognize more classes of objects. While there is a large body of work on explaining image classifiers, there is no published research on how to explain their results, despite the prevalence of object detection use-cases.

For image classifiers, the standard form for an explanation is a subset of highest-ranked pixels that is sufficient for the original classification outcome – typically a small number of contiguous areas. Figure 1 illustrates how this idea is adapted to the output of object detectors: there must exist a separate explanation for each detected object, contained within the bounding box computed by the object detector.

In this paper, we present ANON-REX, an explainability algorithm for object detectors such as YOLO. Explaining the outputs of neural networks is a known hard problem, and it is even harder to explain outputs of object detectors,

as they detect multiple objects in a given image and there are strong performance constraints. We hence introduce aggressive pruning and biased partitioning of the input, as well as the ability to construct explanations of multiple objects in the image simultaneously in order to compute our explanations efficiently.

As there is no existing black-box explainability tool for object detectors, we construct a baseline tool for comparison from ReX, which is an explainability tool for image classifiers [7]. Our experimental results show that ANON-ReX outperforms ReX on YOLO by at least an order of magnitude and is much more scalable with respect to the number of objects detected on the image. Furthermore, our experimental results demonstrate that ANON-ReX produces significantly better explanations than the only existing white-box explainability tool for object detectors, EigenCam-YOLO [18].

To demonstrate that our technique is broadly applicable beyond YOLO, we also present experimental results of ANON-ReX on SSD and Faster R-CNN, both showing similar levels of improvement we observe when using YOLO. Full experimental results, datasets, and the code of ANON-ReX are submitted as a part of the supplementary material.

2. Related Work

Existing algorithms for explaining the output of image classifiers can be roughly divided into black-box algorithms, which are agnostic to the structure of the classifier, and white-box ones, which rely on the access to the internals of the classifier. There are clear advantages to the black-box tools, namely being agnostic to the internal structure and complexity of the classifier. Yet, black-box tools are in general much less efficient than white-box ones, as they rely on querying the classifier many times. Thus, they cannot be used as-is to explain the outputs of object detectors, whose main characteristic is efficiency.

There is a large body of work on algorithms for computing an explanation for a given output of an image classifier. They can be largely grouped into two categories: propagation and perturbation. Propagation-based explanation methods back-propagate a model’s decision to the input layer to determine the weight of each input feature for the decision [4, 19, 25, 26, 28]. Grad-CAM only needs one backward pass and propagates the class-specific gradient into the final convolutional layer of a DNN to coarsely highlight important regions of an input image [23].

Perturbation-based explanation approaches introduce perturbations to the input space directly in search for an explanation. SHAP (SHapley Additive exPlanations) computes Shapley values of different parts of the input and uses them to rank the features of the input according to their importance [17]. LIME constructs a small neural network to

label the original input and its neighborhood of perturbed images and uses this network to estimate the importance of different parts of the input [5, 10, 11, 20, 22]. Finally, ReX (previously called DeepCover) ranks elements of the image according to their importance for the classification and uses this ranking to greedily construct a small explanation [7, 8, 27]. The DeepCover ranking procedure in [27] uses SFL, and is replaced in [7] by the approximate computation of causal responsibility. The latest version, ReX [8], computes multiple explanations for a given input.

None of the tools mentioned above works with YOLO, or any object detector, natively. There exists a version of Grad-CAM for YOLO [3]; unfortunately, however, it is proprietary and not available for experiments. An open source, white-box equivalent is EigenCam-YOLO [1], based on EigenCam [18] and YOLO v8. The approach taken by EigenCam-YOLO works for some images, but often it yields explanations that are too large, highlight the wrong sections of the image, or differ significantly from plain YOLO bounding boxes. A major disadvantage of EigenCam-YOLO is its reliance on heatmaps as its main method of communicating explanations: an image with many identifiable objects, such as the shelf of wine bottles, becomes a red blur when run through EigenCam-YOLO’s explanation algorithm, and the user obtains no further knowledge about the working of the object detector.

3. Overview of ReX

Causal Responsibility eXplanations (ReX) [7, 8] (formerly DeepCover) is an XAI tool based on the solid foundations of causal reasoning [13]. Essentially, ReX constructs an approximation of a causal explanation [13, 14] by first ranking the pixels of a given image according to their importance for the classification, and then constructing an explanation greedily from the saliency landscape of the pixels. The ranking is an approximate degree of responsibility [6], computed on the coarsely partitioned image, and updated by refining the areas of the input with high responsibility, until a sufficiently fine partition is reached.

To compute the degree of responsibility, ReX generates mutants – images with some of the parts masked – and queries the classifier on these mutants. If a non-masked area is sufficient to get the same classification as the original image, it is a cause for the classification, with the degree of responsibility of each part based on the number of parts in the area. For example, if a part by itself is sufficient for the classification, the responsibility of each of its pixels is 1; if, however, the smallest set of parts needed to obtain the same classification is of size 5, then each pixel in each part of this set has the responsibility 1/5.

Essentially, the responsibility is in $[0, 1]$, and the higher it

is, the more important a given pixel is for the classification. If a part has no influence on the classification, the responsibility of each of its pixel is 0, and it is eliminated from further analysis. The process is repeated over a number of different random partitions, and the result is averaged. The partitions are randomly produced, but the precise nature of the random distribution is flexible. ReX supports a number of distributions natively, including discrete uniform and beta-binomial. We use uniform for all of our experiments.

4. ANON-ReX Algorithm

ANON-ReX introduces a number of modifications to the original ReX algorithm, drastically reducing the number of calls to the object detector and building a saliency landscape for multiple objects at the same time. These changes are agnostic to the internals of the object detector, as they change the ReX algorithm only and do not depend on a particular classification or object detection model. There is one caveat to this agnosticism in that different object detector tools return their predictions in different formats. These different formats need to be handled appropriately in order to provide necessary information to ANON-ReX.

We present a high-level view of the algorithm in Figure 2 and its pseudocode in Algorithm 1. Object detection tools return a set of labels and bounding boxes for these labels. We use this initial output as a process queue, which we update and refine during the algorithm. The algorithm maintains a copy of the original set of predictions and bounding boxes separately from the process queue. This allows us to refer back to the initial bounding boxes when extracting explanations from the saliency landscape. An explanation should not extend beyond the borders of the bounding box of the initial prediction (as we see later in Figure 6, allowing explanations to bleed out of the original box results in explanations which are difficult to interpret). The algorithm averages the ranking of pixels over k iterations (for a given parameter k). In each iteration calculating the rank of each pixel in each bounding box,

The *prune* procedure, in combination with the *ranking* procedure, adapted from the one in [7], introduces *aggressive pruning*. Essentially, the algorithm first partitions the input image into s parts and then performs a gradual refinement of the partition based on the *degree of causal responsibility* [6, 13] of each part. The original ReX ranking procedure computes the degree of responsibility of each part and then discards the parts with responsibility 0. In ANON-ReX, we compute the degree of responsibility greedily, and stop at each level when we find a subset of parts whose union (with the remainder of the image masked) elicits the original set of labels from the object detector. All other parts of the bounding box are discarded, and the algorithm progresses to the next refinement level.

The original ReX assumes one object per image, whereas

Algorithm 1 ANON-ReX (x, \mathcal{N})

INPUT: an image x , an object detection model \mathcal{N} , number of iterations k
OUTPUT: a set of explanations \mathcal{E} for each bounding box in $\mathcal{N}(x)$

```

1:  $\mathcal{D} \leftarrow \mathcal{N}(x)$ 
2:  $R \leftarrow \text{map of } 0\text{'s}$ 
3: for  $i$  in  $0 \dots k$  do
4:    $Q \leftarrow \mathcal{D}$ 
5:   initialize all cells of updated to  $-1$ 
6:    $\mathcal{E} \leftarrow \emptyset$ 
7:   while True do
8:      $\mathbb{P} \leftarrow \text{random\_partitions}(Q)$ 
9:     for all  $p \in \mathbb{P}$  do
10:       $m \leftarrow \text{generate\_mutant}(Q, p)$ 
11:       $\text{preds} \leftarrow \mathcal{N}(m)$ 
12:       $(\text{updated}, Q) \leftarrow \text{prune}(\text{preds}, \mathcal{D}, \text{updated})$ 
13:      if  $(\forall u \in \text{updated} : u \geq 0)$  then
14:        break
15:      else if  $(\forall u \in \text{updated} : u = -1)$  then
16:        break
17:      end if
18:    end for
19:  end while
20:   $R \leftarrow R + \text{causal\_ranking}(\text{queue}, \text{updated}, \mathbb{P})$ 
21: end for
22:  $\mathcal{E} \leftarrow \text{extract}(R, \mathcal{D})$ 
23: return  $\mathcal{E}$ 

```

YOLO can produce multiple detections. The procedure Algorithm 2 mutates all bounding boxes detected in the image at the same time. We add the appropriate set of parts of each bounding box to the mutant. For example, assuming 4 parts for each bounding box, Algorithm 2 creates a mutant where each upper left box for every bounding box is revealed in that mutant. We continue this for all combinations of parts for each bounding box.

For reasons of efficiency, we group batches of mutants together. To be concrete, we have the first group of combinations as $(0 \dots s)$, we have each bounding box subdivided into s partitions, numbered appropriately, and we reveal partition s_i for each bounding box to create one mutant. The second group, if required, considers pairs of parts and so on. Grouping in this fashion allows us to balance the benefits of batching (by sending more mutants to the model) without doing too much unnecessary work, *i.e.* considering combinations of partitions when we already have a complete set of passing mutants.

To keep track of which combination of partitions satisfies the classification, we maintain an array the same length as

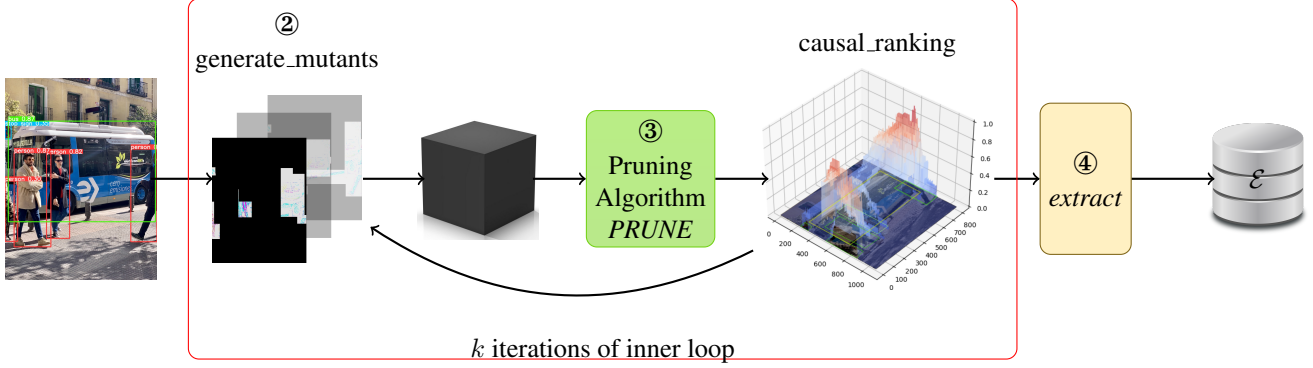


Figure 2. A schematic depiction of our algorithm, returning a set of explanations \mathcal{E} , one for each bounding box in the original image (the black box stands for an object detector). It creates masked mutants for all bounding boxes simultaneously ②, queries the model, then the *pruning algorithm* ③ selects mutants for further investigation and removes all other mutants. ANON-REX then generates a common saliency landscape of pixels for all objects using the causality-based ranking procedure. After k iterations, ④ extracts the explanations from the original bounding boxes and the saliency landscape, returning \mathcal{E} , the set of explanations for all detected objects in the original image.

\mathcal{D} , which holds a combination of parts that is sufficient for a classification (-1 means that none were found). As soon as one such combination is found, we mask all other parts and proceed to partition this combination further. The following claim is straightforward from the procedure.

Claim 1 *At any level, the non-masked parts of the image contain explanations for all detected objects in the image.*

Algorithm 2 *generate_mutant*(Q, p)

INPUT: current process queue Q , and a set of parts p to be unmasked for each bounding box

OUTPUT: a mutant m

- 1: $m \leftarrow \emptyset$
 - 2: **for all** $q \in \text{queue}$ **do**
 - 3: $m \leftarrow m \cup$ (unmask p in bounding box of q)
 - 4: **end for**
 - 5: **return** m
-

There are various subtleties for which we must account. When we mask part of a bounding box and query the model, we do not always get only one prediction in return. For example, if we start with a top-level classification and bounding box of “person” and mask part of that bounding box, we can get a prediction of “person” but also a new bounding box which contains a different classification. We ignore these new bounding boxes and only update the process queue with the bounding box that best matches the prediction and partition which spawned it, as shown in Algorithm 3.

After running a set number of iterations to generate the saliency landscape (Figure 4), the explanation extraction

Algorithm 3 *prune* ($\mathcal{P}, \mathcal{D}, \mathcal{F}$)

INPUT: an array of predictions, *preds*, top-level target predictions \mathcal{D} , a job queue Q , an array *updated*

OUTPUT: *updated*, Q

- 1: **for** *pred* in *preds* **do**
 - 2: **if** (*pred* = original label in \mathcal{D}) **and** (*updated*(*pred*) $\neq -1$) **then**
 - 3: remove all other parts
 - 4: update location in *updated*
 - 5: update Q with *pred*
 - 6: **end if**
 - 7: **end for**
 - 8: **return** (*updated*, Q)
-

procedure extracts explanations for all objects by overlaying bounding boxes produced by YOLO on the landscape and adding in pixels, grouped by responsibility, under the bounding box, until the explanations satisfy the model, as shown in Algorithm 4. We sort all unique responsibility values in the bounding box d under investigation in descending order. We then iterate over these different degrees of responsibility. The procedure *add_pixels_at()* simply reveals all pixels in the image x which are inside the bounding box for d with the appropriate degree of responsibility. We query the model at each responsibility level under the image passes the classifier. This will always succeed as the original bounding box is a passing classification. We reach the original bounding box when we include all pixels with responsibility ≥ 0 . This situation occurs when the bounding box is already minimal for the YOLO classification.

In ANON-REX, extracting explanations from the saliency

Algorithm 4 *extract* ($R, \mathcal{D}, \mathcal{N}, x$)

INPUT: a saliency landscape R , image target detections \mathcal{D} , an object detector \mathcal{N} and an image x
OUTPUT: an array of explanations \mathcal{E}

```
1:  $\mathcal{E} \leftarrow \emptyset$ 
2: for all  $d \in D$  do
3:    $mask \leftarrow \emptyset$ 
4:    $levels \leftarrow unique(R, box(d))$  in descending order
5:   for all  $level \in levels$  do
6:      $mask \leftarrow add\_pixels\_at(x, level, box(d))$ 
7:     if  $\mathcal{N}(mask) = class(d)$  then
8:        $\mathcal{E} \leftarrow \mathcal{E} \cup mask$ 
9:     end if
10:  end for
11: end for
12: return  $\mathcal{E}$ 
```

landscape is complicated not only by presence of bounding boxes, but also by the existence of overlapping bounding boxes. If a smaller bounding box overlaps a larger bounding box and has high responsibility, it will tend to be included into the explanation for the larger box, as the larger box dominates the responsibility landscape. This situation leads to noise in explanations for larger bounding boxes, that is, high ranked pixels that actually contribute to a different label. We handle this problem by treating the bounding boxes as non-intersecting layers in the saliency landscape, hence ensuring that the explanations are not mixed up.

Observation 1 *Explanations found by ANON-ReX might not be the smallest ones.*

It has been observed in the literature that most images contain multiple explanations for their classification [8, 24]. As ANON-ReX finds one explanation per object, which explanations are found depends entirely on the order in which the algorithm computes the degree of responsibility of each part, and hence the output might not be the smallest possible explanation. We note that this issue does not exist in the original ReX ranking procedure. It arises in ANON-ReX due to the aggressive pruning, which allows us to significantly reduce the number of queries to the object detector, as demonstrated in Section 5. An example for such a non-minimal explanation is shown in Figure 3, an explanation for a “person” being this person’s foot. While a correct explanation, it seems more likely that a human would choose a face as an explanation rather than a foot, given an entire picture of a person.



Figure 3. An explanation produced by ANON-ReX for a person in Figure 2. The person’s entire body is present in the original image.

5. Experiments

In this section we present our experimental results for ANON-ReX. We compare ANON-ReX with ReX on the same object detectors, using the number of queries (number of mutant images) as a proxy for performance. Both tools are evaluated on YOLO, SSD, and Faster R-CNN.

	Number of Objects					
	YOLO		SSD		Faster R-CNN	
	10	20	10	13	10	20
baseline	2071	3864	2069	2338	530	4358
ANON-ReX	271	321	483	522	170	751

Table 1. The number of queries (rounded to the nearest integer) produced by the baseline and our tool ANON-ReX for explaining object detector output, using queries as a proxy for performance. We present the results for 10 and for 20 objects, except for SSD, which only recognizes up to 13 objects. Smaller numbers are better.

For all experiments we use the pre-trained yolov8n model [15] on the standard validation dataset ImageNet-mini [2], consisting of 3923 images. If YOLO v8n cannot perform any detection in an image, we exclude that image from consideration. In our experiments, this occurred only for 210 images.

5.1. Analysis of EigenCam-YOLO

A direct comparison with EigenCam-YOLO is challenging, as EigenCam-YOLO only produces heatmaps. Beyond needing post-processing to extract explanations, a heatmap is a not very useful when there is a very large number of bounding boxes in an image. Figure 6a shows a YOLO prediction for an image containing many bottles. The resulting heatmap produced by EigenCam-YOLO is in Figure 6b. Clearly, having almost the whole image marked as “hot” does not provide a lot of insight into the YOLO algorithm.

Our quantitative analysis of EigenCam-YOLO is based on a non-controversial assumption that a good explanation

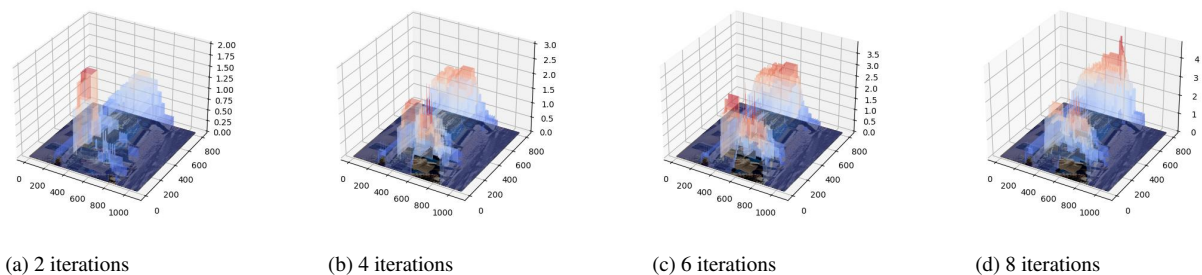


Figure 4. The development of the pixel ranking of the image in Figure 2 over multiple iterations, using discrete uniform for partition creation. YOLO recognizes 6 bounding boxes in this image. We build the ranking for all detections together, then separate them when extracting explanations.

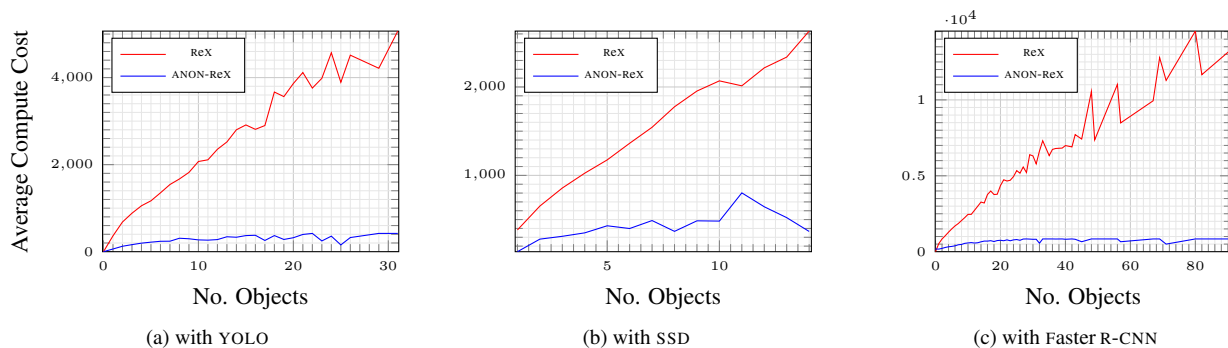


Figure 5. The average number of calls (proxy for performance) produced by ReX (in red) and our tool ANON-ReX (in blue) using three different object detectors on the ImageNet-mini validation dataset. The performance of our tool is largely independent of the number of objects detected in the image. This in contrast to the performance of ReX, which decreases sharply (that is, the number of calls increases) with the increase in the number of objects.

should reside inside the corresponding bounding box, and be at maximum the size of the bounding box. This is because the bounding box contains all the information necessary for the classification, in addition to some extraneous pixels due to the rectangular shape of bounding boxes. In order to measure the efficiency of EigenCam-YOLO’s explanations, we count the number of “hot” pixels detected by EigenCam-YOLO that reside outside of the bounding boxes determined by YOLO, and normalize the count by the total number of pixels in the image. A normalized score of 0 indicates no superfluous pixels, while a normalized score closer to 1 indicates that almost all of the “hot” pixels fall outside of YOLO’s bounding boxes. An example of these superfluous pixels is shown in Figure 7. This particular image was one of the worst detected. We used the validation set from ImageNet-mini for this analysis.

On average, the percentage of “hot” pixels detected in an image by EigenCam-YOLO that fall outside of the YOLO bounding boxes is 30.5%. In other words, about 30% of the explanation created by EigenCam-YOLO for a particular image exceeds the target maximal explanation produced by YOLO. On the basis of this excessive size, we excluded

EigenCam-YOLO from the comparative analysis.

5.2. Experimental results

We use ReX as a baseline black-box explainability tool to which we compare the performance of ANON-ReX. Recall that even black-box tools require a non-trivial adaptation to the output format of object detectors, and to the best of our knowledge, no such adaptations exist. In order to use basic ReX with object detectors, we introduced changes to the input format of ReX without modifying the algorithm. Specifically, for each bounding box detected, we produced a new image in which everything but the bounding box is set to the masking color. We then executed ReX over each independent image (*i.e.*, 6 bounding boxes result in 6 independent runs of ReX). We also added code to process the results of YOLO and SSD, as they are in a different format than the one expected by ReX. Finally, YOLO can produce a “no classification” output, which ReX does not expect. If YOLO is unable to identify anything in the image, we ignore it and do not call ReX on these outputs.

We use the number of mutants generated by both tools as a proxy for performance. As the internal algorithm of

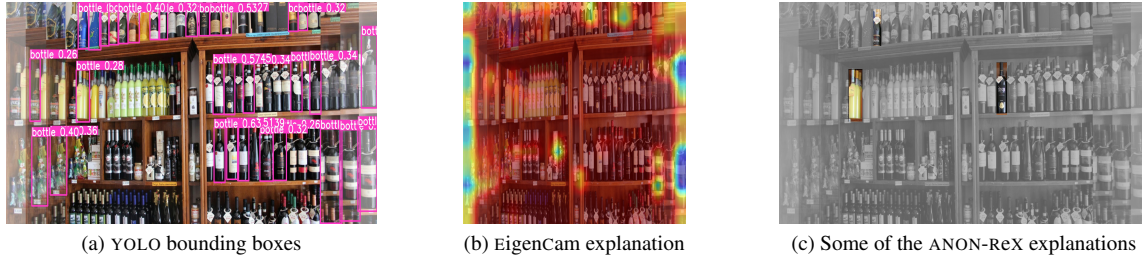


Figure 6. The YOLO bounding boxes 6a and explanations as provided by EigenCam 6b. Due to the large number of bottles, the resulting explanation is almost entirely red. While technically correct, this is not very useful. 6c show a selection of ANON-ReX explanations. Figure 6b has been resized as per the tool’s documentation.

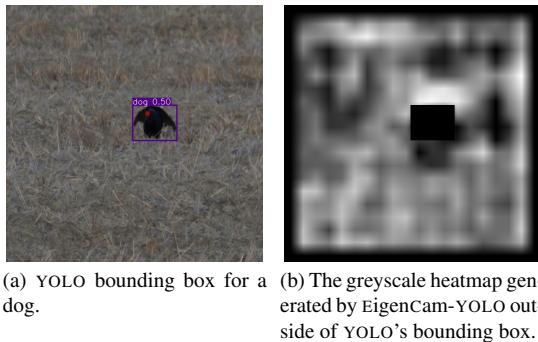


Figure 7. The large proportion of non-black pixels outside the bounding box in 7b shows that EigenCam-YOLO’s explanation takes up the entire image frame, rather than fitting inside the bounding box described by YOLO.

ANON-ReX takes a negligible amount of time, this is a reasonable approximation. In fact, ANON-ReX is faster than ReX even on the same number of mutants, as it also makes much more aggressive use of batching than the original ReX implementation.

Figure 5 shows the average number of mutants produced as a function of the number of objects detected in the image for the three object detectors. Beyond demonstrating the superior performance of ANON-ReX, it also shows that ANON-ReX performance is not affected by the number of objects detected in the image, in contrast to ReX, whose performance rapidly deteriorates with the increase in the number of objects.

A sample of the experimental results is also presented in Table 1, with the performance for images with 10 objects and for 20 objects (except for SSD, where the maximal number of objects is 13), compared to the baseline (ReX). The results show at least an order of magnitude speedup, with ANON-ReX scaling to multiple objects with only a minimal increase in the number of queries.

Remark 1 *The size of produced explanations is often used as a proxy for quality. In our experiments, explanations produced by ANON-ReX are 20.7% larger than those produced*

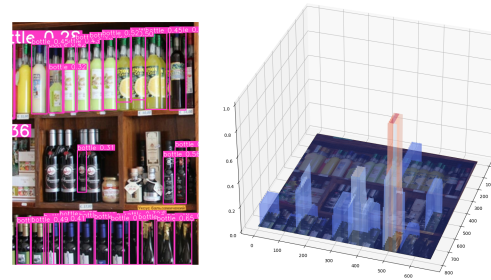


Figure 8. The ANON-ReX pixel ranking for the cropped version of the bottles in Figure 6. YOLO discovers new bottles in the image, but the saliency landscape for the yellow bottles is flat, indicating that no subdivision of the bounding box was detected as a bottle. This in contrast with the colored bottles on the bottom row, all of which have explanations smaller than their original bounding boxes.

by ReX for YOLO, 22.4% larger for SSD, and 52.9% larger for Faster R-CNN. This is partly due to the aggressive pruning, and partly due to object detectors not recognizing small fragments of images as well as image classifiers.

5.3. Explaining images with many objects

Recall that Figure 6a shows a YOLO prediction for an image containing many bottles. ANON-ReX explanations are provided in the form of subsets of pixels, where each subset is sufficient in each bounding box to generate the same label, though not with the same confidence. For the image of many bottles, shown in Figure 6a with the YOLO predictions, Figure 6c shows the explanations generated by ANON-ReX. Of particular interest is the yellow bottle explanation on the left. Closer inspection reveals that there are several bottles in this explanation, not all of them yellow; indeed, on the other yellow bottles in the image, YOLO fails to classify them at all. This may indicate that YOLO is also relying partially on color and not just shape to distinguish a bottle. We cropped the image to include only the section in which YOLO did not identify any objects and re-executed YOLO and ANON-ReX on it. Figure 8 shows that YOLO finds

the yellow bottles on the cropped image. However those have a low confidence, and the saliency landscape for this area is almost completely flat, indicating that there is no explanation for any of these bottles that is smaller than the bounding box itself. This contrasts with the partial, dark, bottles on the bottom row, which have been successfully subdivided at least once, even though they are only partially visible. This indicates YOLO’s dependency on color which, to a human, is orthogonal to recognizing a bottle.

5.4. Shape of explanations

All object detectors we examined produce rectangular bounding boxes. In our experiments, the explanations provided by ANON-ReX were rectilinear, even when the objects do not have straight lines and edges. This may be due to the requirements of YOLO, an insufficient number of iterations from ANON-ReX, or a combination of the two. To investigate this issue, we executed ANON-ReX, with YOLO as the object detector, on a dataset containing images of apples [9]. Apples were chosen as objects without straight lines and ones where the ground truth is known. Figure 1 in the introduction shows an example of some of its outputs. Inspection of the results indicates that even with 20 iterations, the shape of ANON-ReX explanations is strongly influenced by the bounding box requirements. An explanation must be confirmed by the model, and YOLO and similar tools require enough pixels to draw a rectangle, a fundamental part of their classification, thus limiting the shape of the final explanation. On the other hand, ANON-ReX explanations can be much smaller than YOLO bounding boxes, hence providing insights into the YOLO detection process.

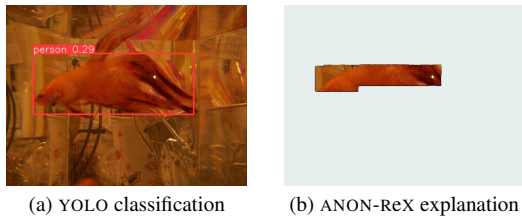


Figure 9. 9b suggests that YOLO misclassifies a fish as a human in 9a, because of the part of the fish that is mistaken for red hair.

5.5. Explaining misclassifications

YOLO, like all models, is not 100% accurate. We analyse two examples of misclassifications and show that their explanations, produced by ANON-ReX, can be helpful in identifying the reasons for misclassification. YOLO recognizes 80 different classes and is capable of returning “no classification” if it does not recognize anything in the image. Figure 9 shows an image of an object that YOLO does not know: a fish. It still provides a very good bounding box detection on the image, with a low confidence, 0.27, that the fish is a

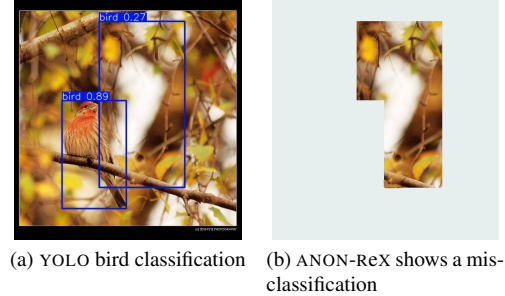


Figure 10. The image in 10a is misclassified as two birds, with the explanation in 10b showing that a branch and white patch in the image are being interpreted as a bird.

person. The ANON-ReX explanation (Figure 9b) highlights the upper region of the fish, suggesting that YOLO is interpreting the image as containing (red) hair. Figure 10 shows an object from a class that YOLO does understand: a bird. Again, we see a bounding box with low confidence labelled bird. The explanation from ANON-ReX is apparently irreducible, being the same size as the original bounding box. YOLO has found something that is plausibly a bird, as the explanation shows both a branch at the bottom of the image (for perching) and a large white shape that swells and contracts much in the fashion of a bird’s body. In our datasets we were unable to identify a misclassification which also had a high confidence.

6. Conclusions

ANON-ReX is the first black box XAI tool for explaining the outputs of object detectors. It significantly outperforms ReX, so the impact of ANON-ReX explanations on the performance of object detectors is much lower, opening the possibility for using ANON-ReX for explainability in real time. We demonstrated the generality of our method and its efficiency by using ANON-ReX on several different object detection tools, both one-pass and two-pass, namely, YOLO, SSD, and Faster R-CNN. We show that existing white box explainability methods, in addition to requiring a significant amount of coding, do not produce sufficiently precise results in terms of quality of explanations.

References

- [1] Eigencam for YOLO v8 interpretability. <https://github.com/rigvedrs/YOLO-V8-CAM>. 2
- [2] Imagenet 1000 (mini). <https://www.kaggle.com/datasets/ifigotin/imagenetmini-1000>. 5
- [3] Kirchknopf Armin, Djordje Slijepcevic, Ilkay Wunderlich, Michael Breiter, Johannes Traxler, and Matthias Zeppelzauer. Explaining YOLO: Leveraging Grad-CAM to explain object detections. 2022. 2
- [4] Sebastian Bach, Alexander Binder, Grégoire Montavon, Frederick Klauschen, Klaus-Robert Müller, and Wojciech Samek. On pixel-wise explanations for non-linear classifier decisions by layer-wise relevance propagation. *PLOS One*, 10(7), 2015. 2
- [5] Jianbo Chen, Le Song, Martin Wainwright, and Michael Jordan. Learning to explain: An information-theoretic perspective on model interpretation. In *International Conference on Machine Learning (ICML)*, pages 882–891. PMLR, 2018. 2
- [6] Hana Chockler and Joseph Y. Halpern. Responsibility and blame: A structural-model approach. *J. Artif. Intell. Res.*, 22:93–115, 2004. 2, 3
- [7] Hana Chockler, Daniel Kroening, and Youcheng Sun. Explanations for occluded images. In *IEEE/CVF International Conference on Computer Vision, ICCV*, pages 1214–1223. IEEE, 2021. 1, 2, 3
- [8] Hana Chockler, David A. Kelly, and Daniel Kroening. Multiple different explanations for image classifiers, 2023. 2, 5
- [9] Samuel Cortinhas. Apples or tomatoes – image classification. <https://www.kaggle.com/datasets/samuelscortinhas/apples-or-tomatoes-image-classification>. 8
- [10] Anupam Datta, Shayak Sen, and Yair Zick. Algorithmic transparency via quantitative input influence: Theory and experiments with learning systems. In *Security and Privacy (S&P)*, pages 598–617. IEEE, 2016. 2
- [11] Ruth Fong, Mandela Patrick, and Andrea Vedaldi. Understanding deep networks via extremal perturbations and smooth masks. In *International Conference on Computer Vision (ICCV)*, pages 2950–2958. IEEE, 2019. 2
- [12] Ross Girshick, Jeff Donahue, Trevor Darrell, and Jitendra Malik. Rich feature hierarchies for accurate object detection and semantic segmentation, 2014. 1
- [13] J. Y. Halpern. *Actual Causality*. MIT Press, Cambridge, MA, 2016. 2, 3
- [14] Joseph Y. Halpern and Judea Pearl. Causes and explanations: A structural-model approach. Part II: Explanations. *British Journal for the Philosophy of Science*, 56(4), 2005. 2
- [15] Glenn Jocher, Ayush Chaurasia, and Jing Qiu. Ultralytics YOLOv8, 2023. 5
- [16] Wei Liu, Dragomir Anguelov, Dumitru Erhan, Christian Szegedy, Scott E. Reed, Cheng-Yang Fu, and Alexander C. Berg. SSD: single shot multibox detector. In *Proceedings of European Conference in Computer Vision ECCV, Part I*, pages 21–37. Springer, 2016. 1
- [17] Scott M. Lundberg and Su-In Lee. A unified approach to interpreting model predictions. In *Advances in Neural Information Processing Systems (NeurIPS)*, pages 4765–4774, 2017. 2
- [18] Mohammed Bany Muhammad and Mohammed Yeasin. Eigen-CAM: Class activation map using principal components. *CoRR*, abs/2008.00299, 2020. 2
- [19] Woo-Jeoung Nam, Shir Gur, Jaesik Choi, Lior Wolf, and Seong-Whan Lee. Relative attributing propagation: Interpreting the comparative contributions of individual units in deep neural networks. In *AAAI Conference on Artificial Intelligence*, pages 2501–2508, 2020. 2
- [20] Vitali Petsiuk, Abir Das, and Kate Saenko. RISE: randomized input sampling for explanation of black-box models. In *British Machine Vision Conference (BMVC)*. BMVA Press, 2018. 2
- [21] Joseph Redmon, Santosh Kumar Divvala, Ross B. Girshick, and Ali Farhadi. You only look once: Unified, real-time object detection. In *Proceedings of CVPR*, pages 779–788, 2016. 1
- [22] Marco Tulio Ribeiro, Sameer Singh, and Carlos Guestrin. “Why should I trust you?” Explaining the predictions of any classifier. In *Knowledge Discovery and Data Mining (KDD)*, pages 1135–1144. ACM, 2016. 2
- [23] Ramprasaath R. Selvaraju, Michael Cogswell, Abhishek Das, Ramakrishna Vedantam, Devi Parikh, and Dhruv Batra. Grad-CAM: Visual explanations from deep networks via gradient-based localization. In *International Conference on Computer Vision (ICCV)*, pages 618–626. IEEE, 2017. 2
- [24] Vivswan Shitole, Fuxin Li, Minsuk Kahng, Prasad Tadepalli, and Alan Fern. One explanation is not enough: Structured attention graphs for image classification. In *Neural Information Processing Systems (NeurIPS)*, pages 11352–11363, 2021. 5
- [25] Avanti Shrikumar, Peyton Greenside, and Anshul Kundaje. Learning important features through propagating activation differences. In *International Conference on Machine Learning (ICML)*, pages 3145–3153. PMLR, 2017. 2
- [26] Jost Tobias Springenberg, Alexey Dosovitskiy, Thomas Brox, and Martin A. Riedmiller. Striving for simplicity: The all convolutional net. In *ICLR (Workshop Track)*, 2015. 2
- [27] Youcheng Sun, Hana Chockler, Xiaowei Huang, and Daniel Kroening. Explaining image classifiers using statistical fault localization. In *ECCV, Part XXVIII*, pages 391–406. Springer, 2020. 2
- [28] Mukund Sundararajan, Ankur Taly, and Qiqi Yan. Axiomatic attribution for deep networks. In *International Conference on Machine Learning*, pages 3319–3328. PMLR, 2017. 2